GeoInformation in Europe, M.A. Gomarsca (ed.)

Model based building reconstruction from InSAR data

A. Thiele, E. Cadario, K. Schulz & U. Thoennessen
FGAN-FOM, Research Institute for Optronics and Pattern Recognition, Ettlingen, Germany

U. Soergel
Institute of Photogrammetry and GeoInformation, Leibniz Universität Hannover, Hannover, Germany

Keywords: urban area, building reconstruction, multi-aspect, InSAR, high-resolution, airborne

ABSTRACT: The improved ground resolution of state-of-the-art synthetic aperture radar (SAR) sensors suggests utilizing SAR data for the analysis of urban areas. The appearance of buildings in SAR data is characterized by the effects of the inherent oblique scene illumination, such as layover, occlusion by radar shadow and multipath signal propagation. Therefore, especially in dense built-up areas, building reconstruction is often impossible from a single measurement alone, but an improvement of the reconstruction quality can be achieved by a combined analysis of multi-aspect data.

The presented approach focuses on reconstruction of the building footprint and detection of the roof type in residential districts supported by knowledge based analysis considering SAR-specific effects. Typical building features like linearity and right-angularity are considered in the model-based approach.

1 INTRODUCTION

The SAR sensor principle requires oblique and side looking illumination of a scene, giving rise to phenomena such as foreshortening, layover, occlusions, total reflection, and multi-bounce scattering. Especially in urban environment, these effects are frequently observed due to vertical walls, tilted roof faces, and in general right-angled structures of buildings. 3D building recognition exploiting these effects has been studied for rural areas (Bolter 2001) and industrial plants (Simonetto *et al.* 2005), (Soergel *et al.* 2001). In high-resolution SAR data, many additional building features become visible which are useful for the analysis (Soergel *et al.* 2006). In Simonetto *et al.* (2005) such data were used for detection and reconstruction of industrial buildings, based on main features observable as L- and T-structures. In Thiele *et al.* (2007) as well L-structures were exploited, combined with the analysis of multi-aspect data from orthogonal flight directions in a residential as well as industrial area.

Beside the L- and T-structures especially in residential areas often parallel line pairs are observable, which can give hints to the roof type. In this paper the appearance of two different roof types is analyzed and the modified result of the L-structure algorithm (Thiele *et al.* 2006) is presented. The reconstruction results, comprising building

footprint, roof type and building height, are visualized and evaluated in comparison with ground truth data, given as LIDAR DSM and orthophoto.

2 APPEARANCE OF FLAT- AND GABLE-ROOFED BUILDINGS

The presented reconstruction approach exploits the multi-bounce scattering between building wall and ground for the detection of the building footprint, and the signature of tilted roof areas as hints for the roof type classification.

In Figure 1 magnitude images are given, covering the same part of the investigated scene from orthogonal views. The red lines in range direction mark a flat- (F) and a gable-roofed (G) building respectively. The corresponding magnitude profiles are depicted in the graphs (b, c, e, f).

Focused on the flat-roofed building, the signature in Figure 1a, b results from illumination to the short building side. Consequently layover area, corner, single roof backscatter and shadow are observable. By contrast the orthogonal illumination (Figure 1d, e) shows layover area, corner and only shadow, because the entire signal of roof is obscured by layover (Thiele *et al.* 2007). The corner, caused by the multi-bounce scattering, is located at the maximum of the magnitude profile.

The magnitude values of gable-roofed building show as well the corner, but in comparison to the flat-roof signature a second maximum is observable in the range profile

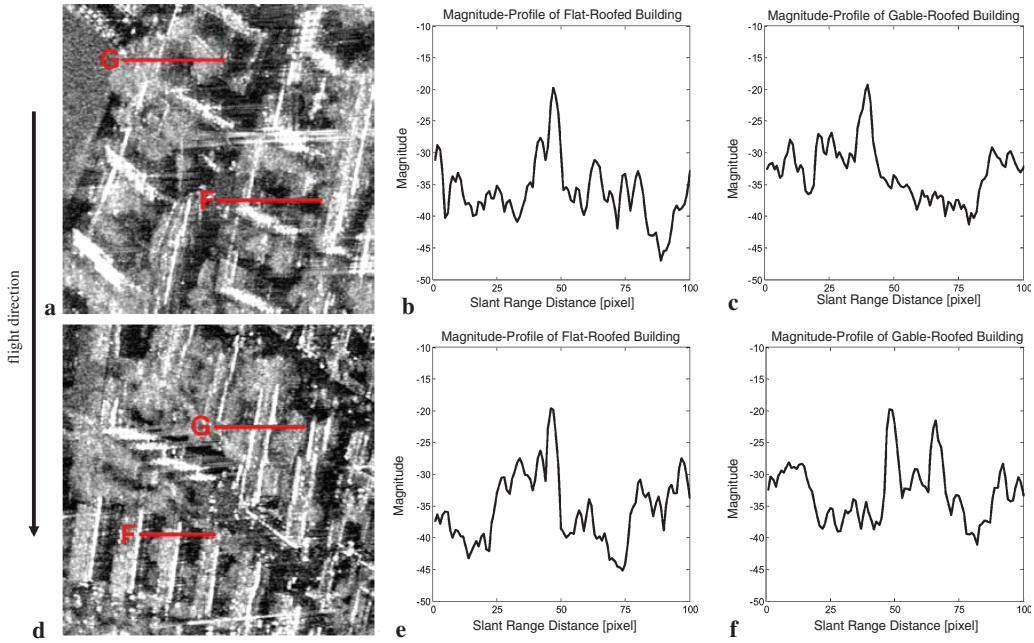

Figure 1. Magnitude image of direction 1 (a) and direction 2 (d) overlaid with red marked range profiles (F – flat-roofed, G – gable-roofed building) given in graphs (flat-roofed – b, e; gable-roofed – c, f).

of illumination direction 2 (Figure 1f). This is caused by summation of whole backscatter signal of the roof area in only few range cells. Of course this phenomenon depends on roof pitch and sensor off-nadir angle, and is only observable if the range direction is approximately orthogonal to the ridge direction. Therefore this second maximum is not observable for direction 1 (Figure 1c), because the profile through the gabled building is nearly parallel to the ridge. A combined analysis of the magnitude and interferometric height images enable the possibility to detect these constellations and distinguish them from other parallel line pairs.

For this study SLC InSAR imagery from Intermap Technologies (Schwaebisch *et al.* 1999) covering a part of the city of Dorsten, Germany, was analyzed. The InSAR data was taken from a single pass interferometric antenna configuration with a spatial resolution of about 38 cm in range and 16 cm in azimuth direction (X-Band). The effective baseline was approx. 2.4 m and the off-nadir angle θ increases from 28° to 52° over swath. The data were taken twice from orthogonal viewing directions, i.e. from each direction two image pairs were recorded. The overlapping area covers five square kilometers of an urban area with a mixture of residential and industrial buildings. The subsequent analysis is focused on a residential part characterized by flat as well as gable-roofed buildings.

3 APPROACH OF BUILDING DETECTION

The approach proposed here is based on lines, because in high-resolution SAR data those are well detectable (Soergel *et al.* 2006). Also Simonetto *et al.* (2005) used such building hints for the reconstruction of industrial buildings by sampling L- and T-structures. There a stereoscopic sequence of SAR images from one aspect was investigated.

The here presented approach is based on the proposed algorithm by Thiele *et al.* (2006) enhanced by a step of roof type detection, tailored for the reconstruction of preferably residential buildings. The searched building model is restricted to a rectangular footprint and a flat respectively gable roof. The reconstruction uses sampled L-structures as building hints caused by double bounce reflection (corner line) and benefits from complementing information of orthogonal views. A discrimination of the generated building candidates concerning the roof type is based on candidate features calculated from the interferometric heights and segmentation results such as parallel lines.

3.1 *Pre-processing*

The pre-processing of the magnitude images includes speckle reduction accomplished with Gamma-Map filter (Lopes *et al.* 1993). The subsequent fusion of the four magnitude images (two antennas, two recording times) comprises a subpixel registration of the images based on coherence maximization. The fusion step is carried out using a maximum operator to concentrate the highest backscatter signal in one image. Before the segmentation of lines using Steger-Operator (Steger *et al.* 1986) a logarithmic scaling is performed.

The formation of the interferometric heights comprises also a subpixel registration. The subsequent interferogram generation includes a multi-look filtering and is followed

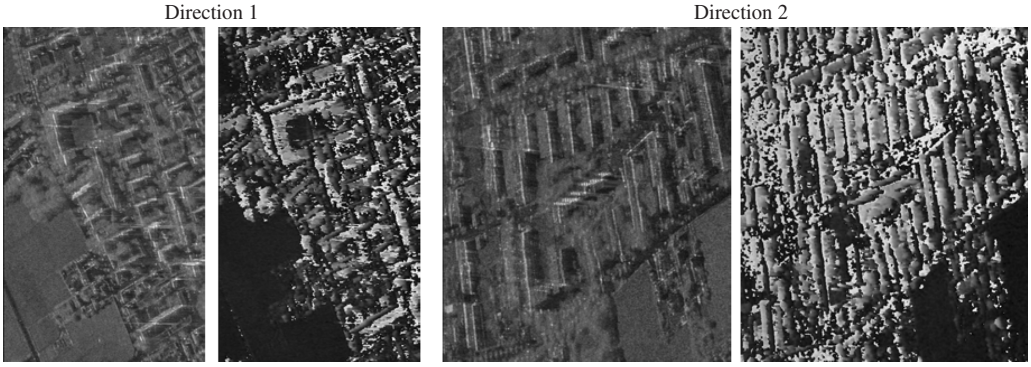

Figure 2. Pre-processed magnitude (left) and interferometric height (right) images of both directions.

by the steps of flat earth compensation, phase centering and phase correction (Thiele *et al.* 2007). The calculated height as well as the magnitude images are shown in Figure 2.

3.2 *Detection of primitives in slant-range geometry*

A corner line shows not the same backscatter characteristic in every image of one direction due to slightly different incidence angles. These changes of backscatter signal are compensated after the maximum fusion. Therefore especially the max-fused image is suitable for the extraction of bright lines using the Steger-Operator. After a linear approximation and subsequent prolongation step straight lines (primitives) are given (Figure 3 left).

For all these primitives a mean value is calculated in their neighborhood regarding interfereometric height values. Due to the fact, that for the reconstruction of the building footprint only lines caused by a dihedral corner reflector between ground and building walls should be considered, a classification of the primitives is necessary. Primitives with a mean height value approximately terrain height are classified to ***corner-line*** primitives

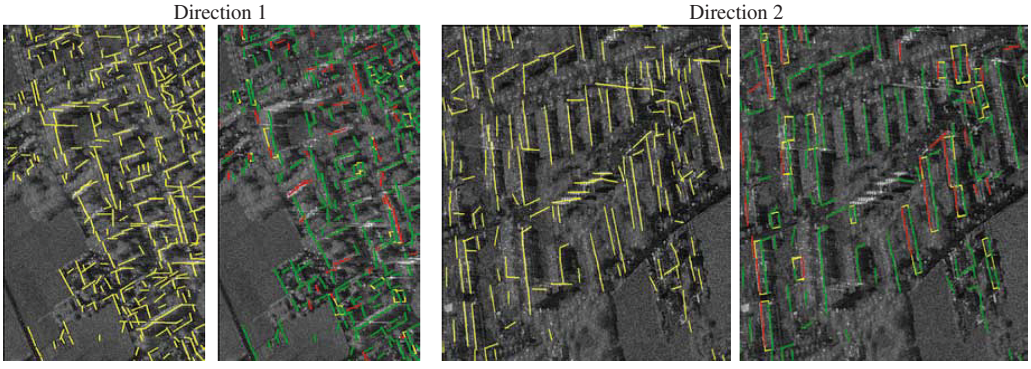

Figure 3. Magnitude images overlaid with all detected lines (yellow, left) and with classified lines (red – layover-line, green – corner-line, right); detected parallel line pairs in yellow(right).

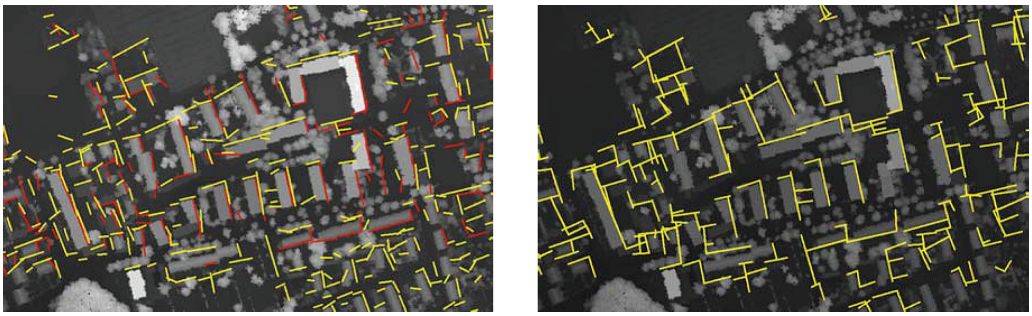

Figure 4. LIDAR-DSM overlaid with projected corner-lines (yellow – direction 1, red – direction 2, left) and with assembled L-structures (yellow, right).

(Figure 3, green marked). Detected bright lines with a higher mean height value are assigned to the group ***layover-lines*** (Figure 3, red marked). Lines which belong to none of these classes are not considered in subsequent work steps.

The classified lines show regular formations parallel to the sensor flight direction. There a layover-line corresponds to the sensor close and a corner-line to the sensor far side of a parallel line pair. This constellation can be a hint to a gable roof as mentioned before in section 2. Therefore all parallel constellations are assembled (Figure 3 yellow) and the gable roof hints are selected.

The resulting corner-line primitives of both flight directions are individually projected from slant range into ground range geometry in the world coordinate system. This projection is performed individually for each primitive using the calculated InSAR heights for every primitive in their surrounding area. In Figure 4 (left) the overlay of reference LIDAR DSM with the primitives of flight direction 1 (yellow) and direction 2 (red) is visualized to show the benefit of multi-aspect data exploitation. These sets of primitives are used for the subsequent building hypotheses generation.

3.3 *Assembly building hypotheses in ground-range geometry*

Starting with the generation of the building footprint the first step comprises the search of line pairs, which must meet angle, bridging and gap tolerances to be an L-structure (Figure 4 right). The union of primitives from both directions reveals the benefit of orthogonal views.

Based on the given flight directions and the sensor orientation a filtering of the extracted L-structures is possible to reduce false alarms (Thiele *et al.* 2007). In the next step parallelograms are derived from the final set of L-structures. Only a subset of the generated parallelograms actually coincide with real buildings, furthermore many competing (overlapping) parallelograms are present. The discrimination step exploits features derived from the related InSAR elevation data (Figure 5 left). The mean height value of the hypotheses has to be some meters above mean terrain height according to the local typical architecture. The subsequent assessment step of the remaining hypotheses valued size of building and mean height of building, and if remaining quadrangles overlap

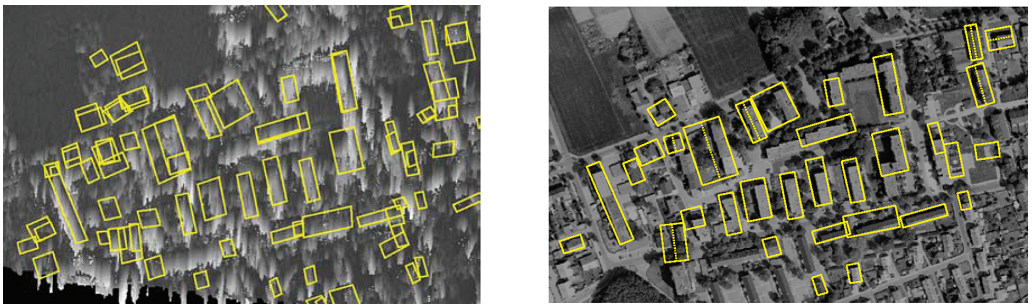

Figure 5. Projected interferometric heights of direction 2 (left) overlaid with filtered building hypotheses; orthophoto (right) overlaid with right-angled footprints of flat- and gable-roofed buildings (ridge: dotted line).

best ratio between these features is taken. For each final building candidate the corresponding right-angled footprint is determined by a minimum bounding rectangle.

The calculation of building height depends on the roof type. As initial type a flat roof is considered, whereas the mean interferometric height $h_{mean\_building}$ inside the building footprint and the mean interferometric terrain height $h_{mean\_terrain}$ defines the building height h_{flat}.

$$h_{flat} = h_{mean\_building} - h_{mean\_terrain}$$

By testing correspondence of footprints and detected parallel lines gable-roofed buildings are assembled (Figure 5 right, ridge: dotted line). The ridge height h_{ridge} and the eave height h_{eave} of this building type are defined as followed, where $h_{max\_\textbf{\textit{layover-line}}}$ is the maximum interferometic height of the ***layover-line***.

$$h_{ridge} = h_{max\_layover-line} - h_{mean_{terrain}} \qquad h_{eave} = h_{ridge} - 2(h_{ridge} - h_{flat})$$

4 RESULTS

The developed approach was applied to an area of the test site Dorsten with a mixture of flat- and gable-roofed buildings. In Figure 5 right an orthophoto is overlaid with the footprints of the reconstructed buildings. The 3D-visualization considering the calculated roof heights is given in Figure 6.

Most of the building footprints are well detected, because the considered SAR phenomena of corner lines exploiting multi-aspect were well observable. In some cases larger footprint of some buildings compared to ground truth is observable, which was also reported in the literature (Gamba *et al.* 2000). This is mainly caused by layover of trees occluding corner lines, giving rise to a tendency of over-sized corner lines. Furthermore some of the small buildings are grouped close together in the ground truth, which leads to a common footprint in the detection result. Furthermore some buildings were not detected

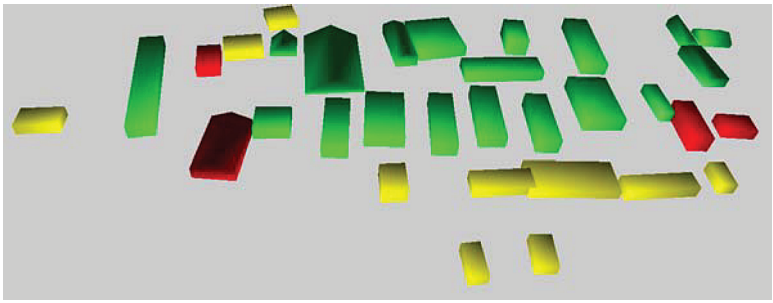

Figure 6. 3D-visualization of final flat- and gable-roofed buildings; green – footprint and roof type correct, yellow – only footprint correct, red – incorrect reconstruction.

because of too close proximity of neighboring buildings and groups of trees resulting in missing L-structures in the data.

The detection of the roof type was correct for all flat-roofed buildings, but some gable-roofed buildings could not be classified right. This can be caused by a wider and lower maximum in the layover area due to the roof pitch or occlusions caused by neighboring trees and buildings. A detailed analysis is planed as future work step.

5 CONCLUSION

The presented approach is focused on the reconstruction of buildings with flat as well as gable roof, which are typically mixed in residential urban areas. A multi-aspect high-resolution InSAR data set was investigated. Depending on the type of building roof, the considered SAR phenomena at building location for the reconstruction were different.

The results achieved by the presented approach show the benefit of a combined analysis of different line constellations (parallel and L-shape line pairs). This is advantageous especially in mixed residential urban areas. A complete reconstruction of every building in the scene was not achieved. This is caused by a lack of segmented primitives (***layover-line*** or ***corner-line***) at building locations, due to overlapping effects between neighboring buildings and trees, in this dense built-up area. A topic of further investigation is the extension of the footprint shape to include more general right-angled outlines besides simple rectangular ones as considered here and a more detailed analysis of parallel line constellations.

REFERENCES

Bolter, R. 2001. *Buildings from SAR: Detection and Reconstruction of Buildings from Multiple View High Resolution Interferometric SAR Data; Ph.D. dissertation, University Graz.*

Gamba, P., Houshmand, B. & Saccini, M. 2000. *Detection and Extraction of Buildings from Interferometric SAR Data; IEEE Transactions on Geoscience and Remote Sensing,* vol. 38, no.1, 2000: 611–618.

Lopes, A., Nezry, E., Touzi, R. & Laur, H. 1993. *Structure detection and statistical adaptive speckle filtering in SAR images; International Journal of Remote Sensing,* vol. 14, no. 9, 1993: 1735–1758.

Schwaebisch, M., Moreira, J. 1999. *The high resolution airborne interferometric SAR AeS-1; Proceedings of the Fourth International Air-borne Remote Sensing Conference and Exhibition, Ottawa, Canada,* 1999: 540–547.

Simonetto, E., Oriot, H. & Garello, R. 2005. Rectangular building extraction from stereoscopic airborne radar images*; IEEE Transactions on Geoscience and Remote Sensing,* vol. 43, no.10, 2005: 2386–2395.

Soergel, U., Schulz, K. & Thoennessen, U. 2001. *Phenomenology-based Segmentation of InSAR Data for Building Detection; in Radig, B., Florczyk, S. (Eds.) Pattern Recognition, 23rd DAGM Symposium, Springer,* 2001: 345–352.

Soergel, U., Thoenessen, U., Brenner, A. & Stilla, U. 2006. *High resolution SAR data: new opportunities and challenges for the analysis of urban areas; IEE Proceedings – Radar, Sonar, Navigation,* 2006.

Steger, C. 1986. An Unbiased Detector of Curvilinear Structures; *IEEE Transactions on Pattern Analysis and Machine Intelligence,* vol. 20, no. 2, 1986: 113–125.

Thiele, A., Cadario, E., Schulz, K., Thoennessen, U. & Soergel, U. 2006. *Building Recognition Fusing Multi-Aspect High-Resolution Interferometric SAR Data;* Proc. IGARSS, 2006, CD ROM.

Thiele, A., Cadario, E., Schulz, K., Thoennessen, U. & Soergel, U. 2007. *Building Recognition from Multi-Aspect High Resolution InSAR Data in Urban Area; IEEE Transactions on Geoscience and Remote Sensing, EUSAR Special Issue,* 2007, in press.